

# Magnetization switching in the $\text{BiFe}_{0.9}\text{Mn}_{0.1}\text{O}_3$ thin films modulated by resistive switching process

Guangyi Chen,<sup>1</sup> Guifeng Bi,<sup>1</sup> Lin Song,<sup>1</sup> Yakui Weng,<sup>2</sup> Danfeng Pan,<sup>1</sup> Yongchao Li,<sup>1</sup> Shuai Dong,<sup>2</sup> Tao Tang,<sup>1</sup> Jun-ming Liu,<sup>1,3</sup> and Jian-guo Wan<sup>1,3,a)</sup>

<sup>1</sup>National Laboratory of Solid State Microstructures and Department of Physics, Nanjing University, Nanjing 210093, China

<sup>2</sup>Department of Physics, Southeast University, Nanjing 211189, China

<sup>3</sup>Collaborative Innovation Center of Advanced Microstructures, Nanjing University, Nanjing 210093, China

(Received 19 July 2016; accepted 5 September 2016; published online 16 September 2016)

Polycrystalline  $\text{BiFe}_{0.9}\text{Mn}_{0.1}\text{O}_3$  thin films have been prepared on Pt/Ti/SiO<sub>2</sub>/Si wafers by a sol-gel process. The film exhibits typical resistive switching (RS) effect. Moreover, accompanied with the RS process, remarkable magnetization switching (MS) behaviors happen, i.e., at low resistance state the film shows high saturation magnetization, while showing low saturation magnetization at high resistance state. We revealed that such a MS effect mainly originates from the conversion of Fe ion valence state between  $\text{Fe}^{2+}$  and  $\text{Fe}^{3+}$  during the RS process, which was confirmed by the x-ray photoelectron spectroscopy measurements. The further first-principle calculations showed that the doping of Mn into the  $\text{BiFeO}_3$  could induce an impurity energy level which makes it facile to achieve the conversion of Fe ion valence state. Based on the conductive filament model, a possible mechanism of tuning the MS effect by RS process is proposed, which is closely related to the conversion of Fe ion valence state along with the forming and rupture of conduction filaments. This work provides us a promising avenue to design switchable multistate devices with both electric and magnetic functionalities. *Published by AIP Publishing.* [<http://dx.doi.org/10.1063/1.4962906>]

The resistive switching (RS) effect in oxides has attracted intense interest in both scientific and industrial fields in recent years due to its versatile advantages, especially its outstanding characteristics in device performance such as high operation speed, high storage density, low power consumption, and nonvolatile features.<sup>1,2</sup> To date, some kinds of material systems have been discovered to exhibit RS effect,<sup>3–5</sup> which generally can be classified into two types, i.e., unipolar resistive switching (URS) effect (e.g., Au/NiO/Pt film<sup>6</sup>) and bipolar resistive switching (BRS) effect (e.g., Pt/CoFe<sub>2</sub>O<sub>4</sub>/Nb:SrTiO<sub>3</sub> heterostructure<sup>7</sup>). For URS effect, several mechanisms have been put forward, and one of the most common accepted mechanisms is the filament model, in which the switching between different resistance states is contributed to the formation and the rupture of conductive filaments in the RS oxides.<sup>8,9</sup> Recently, people found that some other physical phenomena (e.g., the change in magnetization) could appear simultaneously during the RS process, which provides us a possible avenue to design multifunctional devices. For instance, the coexistence of the electric-field-controlled ferromagnetism and the RS behavior was observed in TiO<sub>2</sub> thin films deposited on the Nb:SrTiO<sub>3</sub> single crystal substrates, which may be dominated by the modulation of Schottky-like barrier and the creation/annihilation of oxygen vacancies (OVs).<sup>10</sup> A significant change in magnetization was reported in a La<sub>2/3</sub>Ba<sub>1/3</sub>MnO<sub>3</sub> film with the RS effect, which was attributed to the break/repair of  $-\text{Mn}^{3+}-\text{O}^{2-}-\text{Mn}^{4+}-$  chains.<sup>11</sup>

Herein, we propose another feasible method to tune the magnetism of the RS system based on the modulation of ion

valence state in the oxide. We choose the  $\text{BiFeO}_3$ -based films to demonstrate our idea. It is well known that  $\text{BiFeO}_3$  is a promising multiferroic material because of the coexistence of ferroelectricity and magnetism above room temperature, which has potential and wide applications in the multifunctional devices.<sup>12,13</sup> Recently,  $\text{BiFeO}_3$  also has been experimentally demonstrated to possess the RS effect.<sup>14–17</sup> As previous investigations point out,<sup>18</sup> the RS effect in the  $\text{BiFeO}_3$ -based materials may be accompanied with the valence conversion of Fe ions. Considering the fact that the Fe ion valence in the  $\text{BiFeO}_3$ -based system is connected with the exhibition of its magnetization,<sup>19,20</sup> the change in the magnetism at different RS states may be expected.

In this work, we report on the remarkable modulation of magnetization in the  $\text{BiFe}_{0.9}\text{Mn}_{0.1}\text{O}_3$  (BFMO) thin films by the RS process. Evident variation of magnetization is observed when the film is switched between low and high resistance states. The rate of change in the saturation magnetization between high magnetization state (HMS) and low magnetization state (LMS) can reach as high as ~40%. We reveal that such a magnetization switching (MS) process is dominated by the conversion of Fe ion valence state between  $\text{Fe}^{2+}$  and  $\text{Fe}^{3+}$ , which is accompanied with the formation and the rupture of the conduction filaments during the RS process. Moreover, based on the first-principle calculations, we find that the doping of Mn can make the conversion of Fe ion valence state become more facilely due to the introduction of impurity energy level.

The BFMO thin films were deposited on the commercial Pt/Ti/SiO<sub>2</sub>/Si wafers by a sol-gel process and spin-coating technique.  $\text{Bi}(\text{NO}_3)_3 \cdot 5\text{H}_2\text{O}$ ,  $\text{Fe}(\text{NO}_3)_3 \cdot 9\text{H}_2\text{O}$ , and  $\text{Mn}(\text{CH}_3\text{COO})_2 \cdot 4\text{H}_2\text{O}$  were dissolved in the mixture of 2-Methoxyethanol and

<sup>a)</sup>Author to whom correspondence should be addressed. Electronic mail: wanjg@nju.edu.cn

$\text{CH}_3\text{COOH}$  to make up 0.2 M/l BFMO precursor solution. An excess of 10 mol. %  $\text{Bi}(\text{NO}_3)_3 \cdot 5\text{H}_2\text{O}$  was used to compensate the loss of Bi in the annealing process. The sol solution was spin-coated onto the Pt/Ti/SiO<sub>2</sub>/Si wafers at 600 rpm for 5 s and 6000 rpm for 30 s, then preheated at 280 °C for 5 min. After that, the gel film was annealed at 550 °C for 10 min in O<sub>2</sub> atmosphere by the rapid annealing process. The above process was repeated for five times, finally a BFMO film with 150 nm thickness was obtained. The details of the preparation can be found elsewhere.<sup>18,21</sup> The subsequent X-ray diffraction (XRD) analysis showed that the film was composed of polycrystalline perovskite BFMO phases. (See Figure S1 in the [supplementary material](#).)

For electric treatments, Au top electrodes were sputtered onto the surface of the film. In order to obtain magnetic signals strong enough in the latter magnetic measurements, a large electrode with 1.0 mm in diameter was used in this work. The RS behaviors of the samples were measured using Keithley 2400 sourcemeter at room temperature. To activate the RS effect, we first applied a high voltage to the film for the forming process. When the voltage reached  $\sim 7.2$  V, the film had an abrupt increase in current, indicating that the film was switched to low resistive state (LRS), as shown in Fig. 1(a). To avoid the film from permanent breakdown, we set a current compliance of 500  $\mu\text{A}$ . After the forming process, we measured the RS behaviors. As shown in Fig. 1(b), the sample exhibits typical URS behavior. With increasing the voltage from zero, the current increases fast and gradually reaches a stable LRS (typically,  $\sim 0.1$  A at 1.0 V). When the applied electric voltage increases to 1.4 V, the current drops abruptly, indicating that the film is switched to high resistive state (HRS), which is corresponding to the reset process. Under the HRS, if we apply the electric voltage from zero, an abrupt increase in current will be observed at  $\sim 6.6$  V, indicating that the film is switched to LRS again, which is corresponding to the set process. The repeatability of the RS effect was subsequently examined for the film.

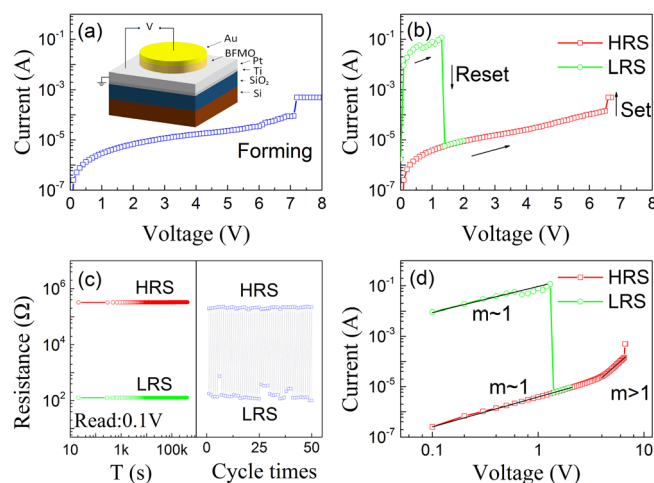


FIG. 1. (a) The forming process of the Au/BFMO/Pt thin film. The inset is a schematic diagram of the sample. (b) The current-voltage curves of the film. The sample shows typical characteristics of the URS effect with clear set and reset processes. (c) Resistance variation with time at HRS and LRS (left side panel), and resistance as a function of cycle number of switching between HRS and LRS (right side panel). The reading voltage is 0.1 V. (d) The current-voltage curve plotted on a log-log scale.

Fig. 1(c) presents the time dependence of resistance state and their evolution in repeated switching. The read voltage was set at 0.1 V. The resistance at HRS is about three orders of magnitude more than that of the LRS. Both HRS and LRS are quite stable even after  $10^3$  s continuous reading, and no significant degradation of resistance within 50 switching cycles. The above results show that the sample has large  $R_{\text{off}}/R_{\text{on}}$  ratio with fairly stable URS characteristics. In addition, we checked the resistance at LRS for the films with smaller electrode area and found that the electrode area had little influence on the resistance at LRS, which is in agreement with the character of filament model. (This model will be discussed in detail in the latter paragraph.)

As mentioned in the beginning, the RS process in the present BFMO thin film may be accompanied with the variation of magnetism. To examine the connection between the RS and possible magnetic change, we measured the room-temperature magnetization behaviors of the BFMO film at different resistance states using the superconducting quantum interference device (SQUID), as shown in Fig. 2(a). The sample exhibits typical ferromagnetic hysteresis loop at all resistance states. The saturation magnetization ( $M_s$ ) value is 19.7  $\text{emu}/\text{cm}^3$  at as-grown state. Interestingly, after the film is switched to LRS or HRS, a remarkable increase in  $M_s$  is observed. For instance, at LRS the film is in high magnetization state (HMS) with a  $M_s$  value of 31.1  $\text{emu}/\text{cm}^3$ ; when the film is switched to HRS, its  $M_s$  value drops to 22.4  $\text{emu}/\text{cm}^3$ ,

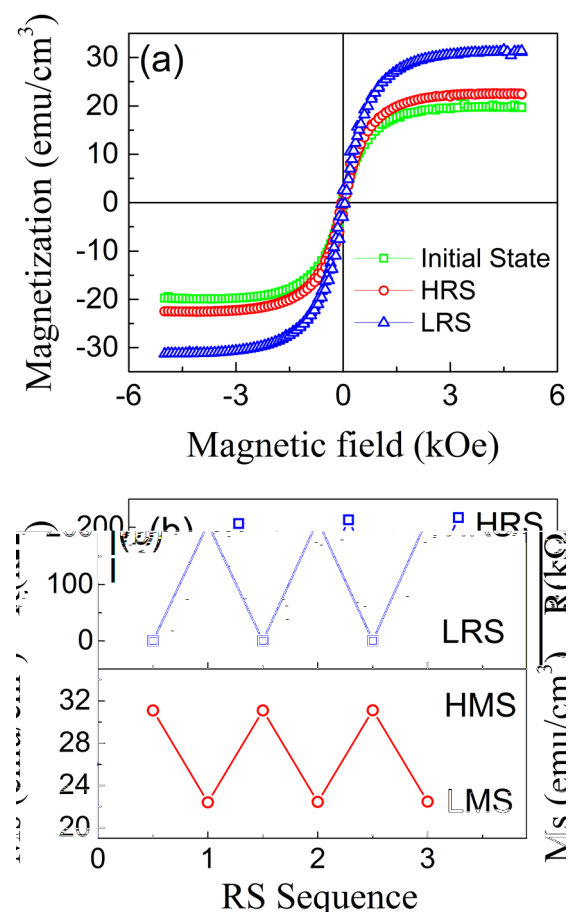


FIG. 2. (a) Room temperature magnetic hysteresis loops of the Au/BFMO/Pt thin film at initial state, LRS, and HRS, respectively. (b) Variations of saturation magnetization ( $M_s$ ) and resistance with the number of RS sequence.

corresponding to the low magnetization state (LMS). Fig. 2(b) further gives the repeatability of such magnetization switching (MS) effect. One observes that the MS effect is repeatable between LRS and HRS. The rate of change in the  $M_s$  value between HMS and LMS maintains a stable value of  $\sim 40\%$ , which is large enough for actual applications. The coexistence of RS and MS effects in one single-phase oxide provides us a fascinating avenue to design switchable multi-state devices with both electric and magnetic functionalities, which has promising potentials in many areas such as multi-channel logic switching, multilevel memory and storage, and multi-field signal detection.

To investigate the magnetism variation at different RS states in the present BFMO thin film, we further analyzed the chemical states at different RS states by performing X-ray photoelectron spectroscopy (XPS) measurements. Before the measurements, we removed the top Au electrodes by Ar ion sputtering at a considerably low energy of 1 keV with the etching time of 300 s. The procedure of XPS characterization of each process is identical and corrected with the C 1s signal. Figs. 3(a)–3(c) present the XPS spectra of Fe 2p at various resistance states. An asymmetric broadband around  $\sim 710.0$  eV is observed in each resistance state. It is known that Fe 2p core level splits into  $2p_{1/2}$  and  $2p_{3/2}$  components in the BiFeO<sub>3</sub>-based film,<sup>22</sup> and the binding energy of Fe  $2p_{3/2}$  is expected to be 710.7 eV for the Fe<sup>3+</sup> while 709.3 eV for the Fe<sup>2+</sup>. The observed asymmetric broadband around  $\sim 710.0$  eV should be the band superposition of both Fe<sup>2+</sup> and Fe<sup>3+</sup>. So we divided the Fe  $2p_{3/2}$  broadband into two subbands centered at 709.3 eV and 710.7 eV, respectively, for each spectrum using the Lorentzian fitting method. In the initial state (Fig. 3(a)), both Fe<sup>2+</sup> and Fe<sup>3+</sup> coexist and the ratio of Fe<sup>2+</sup> to Fe<sup>3+</sup> is about 3:5. The appearance of Fe<sup>2+</sup> in the initial state should be attributed to the high temperature annealing process during the preparation.<sup>18,23,24</sup> A remarkable change in the proportion of Fe<sup>2+</sup> is observed when the RS happens, e.g., at LRS the ratio of Fe<sup>2+</sup> to Fe<sup>3+</sup> arises to about 1:1 (Fig. 3(b)), while 3:4 at HRS (Fig. 3(c)). Previous investigations have demonstrated that the change in

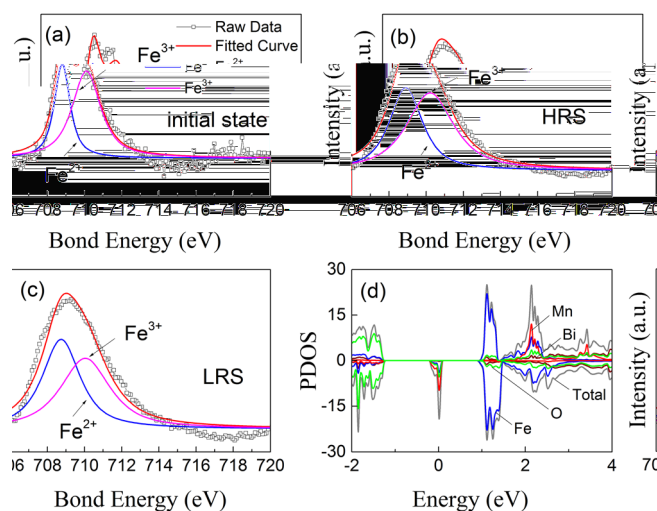


FIG. 3. XPS spectra of Fe $2p_{3/2}$  at (a) initial state, (b) HRS, and (c) LRS. Each spectrum is fitted with the Lorentzian fitting method. (d) Atomic-projected density of states (PDOS) of BiFe<sub>5/6</sub>Mn<sub>1/6</sub>O<sub>3</sub>.

the proportion of Fe<sup>2+</sup> ions in the BiFeO<sub>3</sub>-based film would seriously influence the magnetization of the whole system.<sup>19,20</sup> The Fe<sup>2+</sup> ions not only cause a suppressed inhomogeneous spin structure but also make the canting angle increase and induce a double interaction with Fe<sup>3+</sup> through oxygen.<sup>23</sup> Accordingly, we suggest that the variation of Fe ion valence with the resistance state is crucial to the modulation of magnetism in the present BFMO thin film.

To understand the origin of the valence variation of Fe ions with the resistance state, it is necessary to make a detailed analysis about the electric conduction process and corresponding RS mechanism of the film. Fig. 1(d) plots the current-voltage (I–V) curves of the BFMO thin film at LRS and HRS. Below 1.0 V, the film shows typical Ohmic conduction process ( $I \propto V^m$ ,  $m \sim 1$ ) whether at LRS or HRS. With further increasing the voltage, at LRS the current drops sharply, while at HRS the conduction mechanism turns to be dominated by the space-charge-limited current (SCLC) conduction ( $I \propto V^m$ ,  $m > 1$ ), which is controlled by the localized traps such as oxygen vacancies (OVs). According to the previous investigations, such kind of conductance characteristic is generally accompanied with the formation and rupture of the conductive filaments.<sup>8,17,18,25</sup> In detail, in the forming/set process, a conductive path called as the filament is formed under a suitable voltage, thus the resistive state switches from the initial state/HRS to the LRS. In the reset process, with increasing the applied voltages, the current along the filament path keeps increasing, till reaching a large value. As a result, the filament is ruptured due to the Joule heating effect, and the film is thus switched to HRS.

To further clarify the formation and rupture of the conductive filaments and their correlation with the variation of Fe ion valence states, we drew a simplified schematic diagram for the present BFMO thin film,<sup>18</sup> as shown in Fig. 4. At high voltage (beyond the  $\sim 3.7$  V), the electric conduction process is controlled by the SCLC conduction mechanism in which the oxygen vacancies (OVs) play an important role in determining the electric conduction. During the forming/set

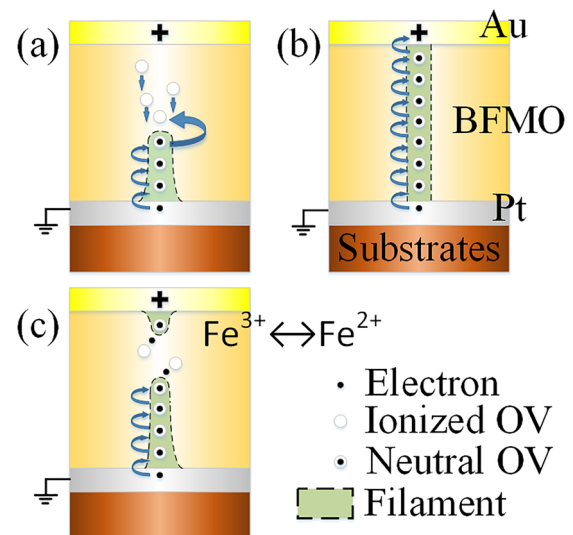


FIG. 4. Schematic diagrams of the RS process and corresponding variations of filament, Fe ion valence state, and oxygen vacancy (OV). (a) and (b) Forming process, (c) Set/reset process.

process, when external electric fields are applied, the electrons are injected into the film; meanwhile, the ionized OV's tend to migrate locally and align along the direction of electric fields (Fig. 4(a)). These ionized OV's act as electron trapping centers and capture electrons to neutralize the local charges, which causes partial  $\text{Fe}^{3+}$  ions in the vicinity of OV's are reduced into  $\text{Fe}^{2+}$ . The  $\text{Fe}^{2+}$  ions not only induce local distortion but also make the electric conduction easier. The combination of capturing electrons by OV's and the formation of  $\text{Fe}^{2+}$  ions cause the filaments to be built,<sup>18,22</sup> so the sample switches into the LRS (Fig. 4(b)), accompanied with the enhancement of magnetization due to the increase in  $\text{Fe}^{2+}$  ions. During the reset process, when the applied voltage reaches a higher value, the heating effect produced by the current will cause the thermally assisted desorption of electrons from the OV's, so the conductive filament is ruptured and the electrons captured by OV's are released. In this process, the OV's recover initial ionized state and  $\text{Fe}^{2+}$  ions go back to  $\text{Fe}^{3+}$ . Therefore, the sample is switched back to HRS and its magnetization decreases (Fig. 4(c)). Finally, as aforementioned, since the MS effect relies on the formation and rupture of conduction filaments which can be repeated stably, a good retention of MS effect in the present BFMO thin film may be expected.

The doping of Mn into the  $\text{BiFeO}_3$  also plays an important role in the process of RS and MS, which makes both of them be accomplished more easily. The valence states of Mn ions at different resistance states are presented in the [supplementary material](#) (Figure S2). We calculated the average valence state of Mn ions, and obtained 3.01 at LRS and 3.02 at HRS, both of which are very close to each other. This rough result implies that the doping of Mn may have little influence on the variation of total magnetization at different resistance states though the actual situation is more complicated. However, our first-principles calculation results shown in Fig. 3(d) confirm that the doping of Mn ions can make the conversion of the Fe ion valence state between  $\text{Fe}^{2+}$  and  $\text{Fe}^{3+}$  become easier. To simplify the calculations, a  $\text{BiFe}_{5/6}\text{Mn}_{1/6}\text{O}_3$  supercell was used in this work. From the atomic-projected density of states (PDOS) in Fig. 3(d), one observes that the electronic structure of the Mn-doped  $\text{BiFeO}_3$  is significantly modulated comparing with the parent  $\text{BiFeO}_3$ , i.e., a distinct impurity energy level near the Fermi level appears in the forbidden band of  $\text{BiFeO}_3$ . Such a change in the electronic structure not only makes the conversion between  $\text{Fe}^{2+}$  and  $\text{Fe}^{3+}$  be accomplished facily but also is helpful for the formation of conductive filament path between the electrodes.

In conclusion, polycrystalline  $\text{BiFe}_{0.9}\text{Mn}_{0.1}\text{O}_3$  thin films have been prepared on the Pt/Ti/SiO<sub>2</sub>/Si wafers by a sol-gel process. The film exhibits evident MS effect when the resistance state is switched between LRS and HRS. The XPS results confirm that the film has an evident change in the Fe ion valence when the resistance state changes. The first-principle calculations show that the doping of Mn can induce an impurity energy level which makes the realization of both RS and MS processes more easily. A possible mechanism of tuning the MS effect in the present BFMO film with RS

effect is proposed, which is closely connected with the conversion of Fe ion valence states. The coexistence of MS and RS effect in a single-phase oxide provides us a promising avenue to design switchable multistate devices with both electric and magnetic functionalities.

See [supplementary material](#) for the XRD pattern of the BFMO thin film, the XPS spectra of Mn in the BFMO thin film at different resistance states, and the theoretical simulation of  $\text{BiFe}_{5/6}\text{Mn}_{1/6}\text{O}_3$  using the first-principles method.

This work was supported by the National Key Research Programme of China (Grant No. 2016YFA0201004), the National Key Projects for Basic Research of China (Grant No. 2015CB921203), and the National Natural Science Foundation of China (Grant Nos. 51472113 and 11134005).

- <sup>1</sup>R. Waser, R. Dittmann, G. Staikov, and K. Szot, *Adv. Mater.* **21**, 2632 (2009).
- <sup>2</sup>R. Waser and M. Aono, *Nat. Mater.* **6**, 833 (2007).
- <sup>3</sup>A. Q. Jiang, C. Wang, K. J. Jin, X. B. Liu, J. F. Scott, C. S. Hwang, T. A. Tang, H. B. Lu, and G. Z. Yang, *Adv. Mater.* **23**, 1277 (2011).
- <sup>4</sup>J. C. Scott and L. D. Bozano, *Adv. Mater.* **19**, 1452 (2007).
- <sup>5</sup>J. Choi, J. S. Kim, I. Hwang, S. Hong, I. S. Byun, S. W. Lee, S. O. Kang, and B. H. Park, *Appl. Phys. Lett.* **96**, 262113 (2010).
- <sup>6</sup>Y. Q. Xiong, W. P. Zhou, Q. Li, M. C. He, J. Du, Q. Q. Cao, D. H. Wang, and Y. W. Du, *Appl. Phys. Lett.* **105**, 032410 (2014).
- <sup>7</sup>Q. W. Wang, Y. D. Zhu, X. L. Liu, M. Zhao, M. C. Wei, F. Zhang, Y. Zhang, B. L. Sun, and M. Y. Li, *Appl. Phys. Lett.* **107**, 063502 (2015).
- <sup>8</sup>M. C. Chen, T. C. Chang, C. T. Tsai, S. Y. Huang, S. C. Chen, C. W. Hu, S. M. Sze, and M. J. Tsai, *Appl. Phys. Lett.* **96**, 262110 (2010).
- <sup>9</sup>W. Eerenstein, N. D. Mathur, and J. F. Scott, *Nature* **442**, 759 (2006).
- <sup>10</sup>S. Q. Ren, H. W. Qin, J. P. Bu, G. C. Zhu, J. H. Xie, and J. F. Hu, *Appl. Phys. Lett.* **107**, 062404 (2015).
- <sup>11</sup>Y. Q. Xiong, W. P. Zhou, Q. Li, Q. Q. Cao, T. Tang, D. H. Wang, and Y. W. Du, *Sci. Rep.* **5**, 12766 (2015).
- <sup>12</sup>G. Catalan and J. F. Scott, *Adv. Mater.* **21**, 2463 (2009).
- <sup>13</sup>H. Bea, M. Bibes, F. Ott, B. Dupe, X. H. Zhu, S. Petit, S. Fusil, C. Deranlot, K. Bouzehouane, and A. Barthelemy, *Phys. Rev. Lett.* **100**, 017204 (2008).
- <sup>14</sup>K. B. Yin, M. Li, Y. W. Liu, C. L. He, F. Zhuge, B. Chen, W. Lu, X. Q. Pan, and R. W. Li, *Appl. Phys. Lett.* **97**, 042101 (2010).
- <sup>15</sup>X. J. Zhu, F. Zhuge, M. Li, K. B. Yin, Y. W. Liu, Z. H. Zuo, B. Chen, and R. W. Li, *J. Phys. D: Appl. Phys.* **44**, 415104 (2011).
- <sup>16</sup>C. H. Yang, J. Seidel, S. Y. Kim, P. B. Rossen, P. Yu, M. Gajek, Y. H. Chu, L. W. Martin, M. B. Holcomb, Q. He, P. Maksymovych, N. Balke, S. V. Kalinin, A. P. Baddorf, S. R. Basu, M. L. Scullin, and R. Ramesh, *Nat. Mater.* **8**, 485 (2009).
- <sup>17</sup>M. Li, F. Zhuge, X. Zhu, K. Yin, J. Wang, Y. Liu, C. He, B. Chen, and R. W. Li, *Nanotechnology* **21**, 425202 (2010).
- <sup>18</sup>J. M. Luo, S. P. Lin, Y. Zheng, and B. Wang, *Appl. Phys. Lett.* **101**, 062902 (2012).
- <sup>19</sup>W. Eerenstein, F. D. Morrison, J. Dho, M. G. Blamire, J. F. Scott, and N. D. Mathur, *Science* **307**, 1203 (2005).
- <sup>20</sup>J. Wang, A. Scholl, H. Zheng, S. B. Ogale, D. Viehland, D. G. Schlom, N. A. Spaldin, K. M. Rabe, M. Wuttig, L. Mohaddes, J. Neaton, U. Waghmare, T. Zhao, and R. Ramesh, *Science* **307**, 1203 (2005).
- <sup>21</sup>S. K. Singh, H. Ishiwara, K. Sato, and K. Maruyama, *J. Appl. Phys.* **102**, 094109 (2007).
- <sup>22</sup>Y. Wang, Q. H. Jiang, H. C. He, and C. W. Nan, *Appl. Phys. Lett.* **88**, 142503 (2006).
- <sup>23</sup>F. Z. Huang, X. M. Lu, W. W. Lin, Y. Kan, J. T. Zhang, Q. D. Chen, Z. Wang, L. B. Li, and J. S. Zhu, *Appl. Phys. Lett.* **97**, 222901 (2010).
- <sup>24</sup>F. Z. Huang, X. M. Lu, W. W. Lin, X. M. Wu, Y. Kan, and J. S. Zhu, *Appl. Phys. Lett.* **89**, 242914 (2006).
- <sup>25</sup>K. M. Kim, B. J. Choi, M. H. Lee, G. H. Kim, S. J. Song, J. Y. Seok, J. H. Yoon, S. Han, and C. S. Hwang, *Nanotechnology* **22**, 254010 (2011).